JPE 9-4-15

Input-Output Feedback Linearization of Sensorless IM Drives with Stator and Rotor Resistances Estimation

Masood Hajian†, Jafar Soltani*, Gholamreza Arab Markadeh**, and Saeed Hosseinnia*

†*Dept. of Electrical and Computer Eng., Isfahan University of Technology, Isfahan, Iran
**Eng. Department, Shahrekord University, Shahrekord, Iran

ABSTRACT

Direct torque control (DTC) of induction machines (IM) is a well-known strategy of these drives control which has a fast dynamic and a good tracking response. In this paper a nonlinear DTC of speed sensorless IM drives is presented which is based on input-output feedback linearization control theory. The IM model includes iron losses using a speed dependent shunt resistance which is determined through some effective experiments. A stator flux vector is estimated through a simple integrator based on stator voltage equations in the stationary frame. A novel method is introduced for DC offset compensation which is a major problem of AC machines, especially at low speeds. Rotor speed is also determined using a rotor flux sliding-mode (SM) observer which is capable of rotor flux space vector and rotor speed simultaneous estimation. In addition, stator and rotor resistances are estimated using a simple but effective recursive least squares (RLS) method combined with the so-called SM observer. The proposed control idea is experimentally implemented in real time using a FPGA board synchronized with a personal computer (PC). Simulation and experimental results are presented to show the capability and validity of the proposed control method.

Keywords: Induction Motor, Direct Torque Control, Input-Output, Stator Flux, Sliding Mode, RLS

1. Introduction

Induction drive control techniques are well treated in the literature. Field orientation control (FOC) and direct torque control methods appear to be very convenient for good dynamic performance operation [1-4]. DTC has a faster dynamic response due to the absence of the PI current controllers. However, conventional DTC methods based on hysteresis or bang-bang controllers have some serious drawbacks such as a high amount of torque and flux pulsations and variable switching frequency of the PWM inverter [5,6].

To overcome these drawbacks, many researchers have tried to propose different DTC schemes with constant switching frequency over the last two decades [7,8].

The parametric deviation in all mentioned methods significantly affects the dynamic performance and even the stability of practical implementation. Therefore, for

Manuscript received Jan 5, 2009; revised June 9, 2009
†Corresponding Author: m.hajian@ec.iut.ac.ir
Tel: +98- 311- 391- 2450, Fax: +98- 311- 391-2451, Isfahan Univ
*Dept. of Electrical and Computer Eng., Isfahan University of Technology, Iran
**Eng. Department, Shahrekord University, Shahrekord, Iran

nonlinear feedback control of induction motors, many studies have recently presented useful compensators for the influence of the motor parameters' variations [7-11].

The principles of predictive control, direct torque control and space vector modulation (SVM) technique for a sensorless IM drive have been combined and applied to an induction motor drive in [7]. Based on this method, the torque error signal and the stator flux reference are delivered to a predictive controller which produces the required voltage command. A complicated Lyapunov based stator flux observer is also proposed in [7] in order to estimate the rotor speed, rotor and stator resistances and stator flux vector simultaneously. The proposed robust method of [7] is dependent on a complex thirteenth order stator flux observer which is very difficult for practical implementation.

In [9], a DTC sliding mode control has been described for a speed sensorless IM drive. The control scheme of [9] is based on the combination of SM control and stator flux field orientation control of an IM drive. The DTC-SVM scheme of [9] needs frame transformation from the stationary reference frame to the stator flux field orientation coordinate frame and vice versa; therefore, it has a relatively high computation time. Moreover, since the vector control scheme is, in fact, an input-output feedback linearization method, it has internal dynamics which cannot be analytically proven to be stable under the transient and steady state conditions. This means that the control system is only locally stable if the controller gains are properly adjusted.

In this paper, considering the motor iron losses, a DTC-SVM method is introduced for speed sensorless three-phase IM drives which is designed in the stationary reference frame. According to this method, the error signals of the torque and stator flux references with respect to their actual values are delivered to the non-linear controller which is developed based upon an input-output feedback linearization technique. The total stability of the so-called controller is proven through the Lyapunov theory. The stator flux space vector is determined using a pure integrator based on stator voltage equations in the stationary coordinate frame. One may note that the most significant problem with this estimation method is that the effects of dc offset exist in the measured voltage and current signals.

The most common solution presented for dc offset compensation is the replacement of the stator flux integrator by a low-pass filter. The limited dc gain of such a low-pass filter eases this problem as long as the stator frequency is much greater than the filter cutoff frequency; however, the phase shift is produced between the pure integrator and low-pass filter, which determines the field angle error, especially at low speeds [12].

Holtz et al. proposed a contribution to the offset voltage vector as the time average of the maximum and minimum points of the stator flux vector [12]. It is worthwhile to mention that absolute values of the so-called maximum and minimum points are restricted to the motor reference flux and, hence, the method is not capable of compensation in the presence of high and medium values of voltage and current dc offsets. Moreover, precise detection of maximum and minimum values of stator flux vector components requires almost a heavy signal processing procedure because harmonic components exist in the measured and calculated quantities.

An improved method of integration has been proposed in [13], where the stator flux vector angle is forced to lag the motor induced voltage using a closed loop PI controller. Although this method seems to be a correct solution in principle, the magnitude of the induced voltage becomes extremely small at very low speeds, which makes dc offset and other disturbances comparable with the main voltage. Moreover, the dynamic delay of the closed-loop control suggested for error correction is another problem of this method.

A novel method is proposed in this paper to compensate for the effective value of existing dc offsets on the sampled signals without any considerable phase lag. For this purpose, the equivalent existing dc offset on the two axis components of the IM internal voltage space vector in the stationary reference frame is calculated on-line and compensated before integration. It should be noted that the motor phase voltage sensors have been eliminated and a simple but effective method is introduced for phase voltage estimation using the dc link voltage and time assignments of the SVM inverter.

The IM speed sensorless adaptive control is the final objective of this research work. Elimination of mechanical sensors increases the system reliability while decreasing the total drive cost. However, the IM speed sensorless schemes are extremely sensitive to motor parameter variations, especially to rotor and stator resistances that change with temperature and skin effects. In addition, steady state error will exist in the motor flux estimation if these parameters are not perfectly detected. So far, many research methods such as model reference adaptive system (MRAS) based, Lyapunov-based, extended Kalman filter (EKF) based or artificial intelligence (AI) based observers have been proposed for motor resistances estimation [14-16].

In this paper, a rotor flux SM observer is proposed which is capable of simultaneous rotor flux and rotor speed estimation so that the persistency of excitation (PE) condition is satisfied. A simple but effective RLS-based estimator is also introduced and combined with the so-called observer for synchronic determination of stator and rotor resistances.

The feasibility and capability of the proposed control approach is supported by simulation and experimental results.

2. IM DTC-SVM Scheme

Considering the IM equivalent core losses through a speed dependent shunt resistance (R_c) in the stationary reference frame as depicted in Fig. 1, the IM fifth order model with stator fluxes ($\lambda_{\alpha s}$, $\lambda_{\beta s}$), stator currents ($i_{\alpha s}$, $i_{\beta s}$) and rotor speed (ω_r) as state variables is derived as [17].

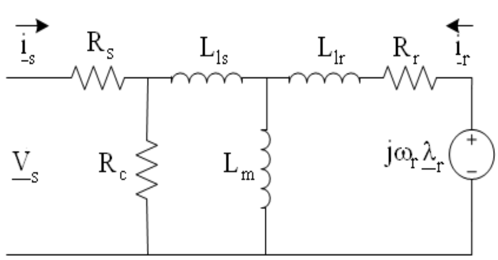

Fig. 1. IM equivalent circuit in the stationary reference frame.

$$\frac{d}{dt}\underline{\mathbf{x}} = \mathbf{A}\underline{\mathbf{x}} + \mathbf{B}\underline{\mathbf{v}}_{\mathbf{s}}$$

$$\frac{d}{dt}\omega_r = \frac{n_p}{J_r}(T_e - T_l) - \frac{B_r}{J_r}\omega_r$$

with,

$$\underline{\mathbf{x}} = \begin{bmatrix} \underline{\boldsymbol{\lambda}}_{\mathbf{s}} \\ \underline{\mathbf{i}}_{\mathbf{s}} \end{bmatrix} \;,\; \underline{\boldsymbol{\lambda}}_{\mathbf{s}} = \begin{bmatrix} \lambda_{\alpha s} \\ \lambda_{\beta s} \end{bmatrix} \;,\; \underline{\mathbf{i}}_{\mathbf{s}} = \begin{bmatrix} i_{\alpha s} \\ i_{\beta s} \end{bmatrix},$$

$$\underline{\mathbf{v}}_{\mathbf{s}} = \left(\frac{R_c}{R_c + R_s}\right)\begin{bmatrix} v_{\alpha s} \\ v_{\beta s} \end{bmatrix} \;,\; Te = \frac{3}{2} n_p \left(\underline{\boldsymbol{\lambda}}_{\mathbf{s}} \times \underline{\mathbf{i}}_{\mathbf{s}}\right)$$

$$\mathbf{A} = \begin{bmatrix} \mathbf{A_{11}} & \mathbf{A_{12}} \\ \mathbf{A_{21}} & \mathbf{A_{22}} \end{bmatrix} \;,\; \mathbf{B} = \begin{bmatrix} \mathbf{B_1} \\ \mathbf{B_2} \end{bmatrix}$$

$$\mathbf{A_{11}} = \mathbf{0_{2\times2}} \;,\; \mathbf{A_{12}} = -(R_s \parallel R_c)\mathbf{I_{2\times2}}$$

$$\mathbf{A_{21}} = -\frac{R_r}{\sigma L_m^2}\mathbf{I_{2\times2}} + \frac{\omega_r L_r}{\sigma L_m^2}\mathbf{J_{2\times2}}$$

$$\mathbf{A_{22}} = -\frac{R_r L_s + (R_s \parallel R_c)L_r}{\sigma L_m^2}\mathbf{I_{2\times2}} + \omega_r \mathbf{J_{2\times2}}$$

$$\mathbf{B_1} = \begin{bmatrix} 1 \\ 1 \end{bmatrix}, \mathbf{B_2} = \begin{bmatrix} -\dfrac{L_r}{\sigma L_m^2} \\ -\dfrac{L_r}{\sigma L_m^2} \end{bmatrix}, \mathbf{I_{2\times2}} = \begin{bmatrix} 1 & 0 \\ 0 & 1 \end{bmatrix}, \mathbf{J_{2\times2}} = \begin{bmatrix} 0 & -1 \\ 1 & 0 \end{bmatrix} \tag{1}$$

where, R_c has been taken close to the stator resistance for greater simplicity. L_s and L_r are the stator and rotor inductances, L_m is the magnetizing inductance, $\sigma = 1 - \frac{L_m^2}{L_s L_r}$ is the leakage coefficient, R_s , R_r and T_r are the stator and rotor resistances and rotor time constant, respectively, while n_p shows the number of pole pairs. T_e, T_l, B_r and J_r are also motor electromagnetic torque, load torque, rotational friction coefficient and total moment of inertia, respectively.

The control objective is the tracking of motor electromagnetic torque T_e and stator flux magnitude $|\underline{\boldsymbol{\lambda}}_{\mathbf{s}}|$ which is achieved as the following.

$$\underline{\boldsymbol{\xi}} = \underline{\boldsymbol{\Delta}} - \boldsymbol{\Delta}_{\mathbf{r}} \;,\; \underline{\boldsymbol{\xi}} = \begin{bmatrix} \xi_1 \\ \xi_2 \end{bmatrix}, \underline{\boldsymbol{\Delta}} = \begin{bmatrix} T_e \\ |\underline{\boldsymbol{\lambda}}_{\mathbf{s}}|^2 \end{bmatrix}, \boldsymbol{\Delta}_{\mathbf{r}} = \begin{bmatrix} T_{er} \\ |\lambda_{sr}|^2 \end{bmatrix} \tag{2}$$

where, λ_{sr} is the stator reference flux and T_{er} is the reference value of the motor electromagnetic torque. The error dynamics of this system are obtained as

$$\dot{\underline{\xi}} = \underline{\mathbf{f}}(\underline{\mathbf{x}}) + \mathbf{C}\underline{\mathbf{u}}$$

$$\underline{\mathbf{f}}(\underline{\mathbf{x}}) = \begin{bmatrix} F_{tr} \\ F_{\lambda s} \end{bmatrix}, \mathbf{C} = \begin{bmatrix} 1 & 0 \\ 0 & 1 \end{bmatrix} \tag{3}$$

$$\underline{\mathbf{u}} = \frac{R_c}{R_c + R_s} \begin{bmatrix} \frac{3}{2} n_P (i_{\beta s} + \frac{L_r}{\sigma L_m^2} \lambda_{\beta s}) & -\frac{3}{2}(i_{\alpha s} + \frac{L_r}{\sigma L_m^2} \lambda_{\alpha s}) \\ 2\lambda_{\alpha s} & 2\lambda_{\beta s} \end{bmatrix} \begin{bmatrix} v_{\alpha s} \\ v_{\beta s} \end{bmatrix} \tag{4}$$

where the functions F_{tr} and $F_{\lambda s}$ are

$$F_t = \frac{3}{2} n_P [\frac{\omega_r L_r}{\sigma L_m^2}(\lambda_{\alpha s}^2 + \lambda_{\beta s}^2) + \frac{1}{\sigma L_m^2}(R_r L_s + (R_s \| R_c) L_r)$$
$$(\lambda_{\alpha s} i_{\beta s} - \lambda_{\beta s} i_{\alpha s}) + \omega_r (\lambda_{\alpha s} i_{\alpha s} + \lambda_{\beta s} i_{\beta s})] - \frac{d}{dt} T_{er}$$
$$F_{\lambda s} = -2(R_s \| R_c)(\lambda_{\alpha s} i_{\alpha s} + \lambda_{\beta s} i_{\beta s}) - 2\lambda_{sr} \frac{d}{dt} \lambda_{sr} \tag{5}$$

The control effort should be chosen in such a manner that the Lyapunov function candidate satisfies the Lyapunov stability criteria

$$V = \frac{1}{2} \underline{\xi}^{\mathbf{T}} \underline{\xi} > 0 \tag{6}$$

This can be assured for

$$\dot{V} = \underline{\xi}^{\mathbf{T}} \mathbf{\Gamma} \underline{\xi} < 0 \tag{7}$$

where, $\mathbf{\Gamma} = \begin{bmatrix} \alpha_t & 0 \\ 0 & \alpha_{\lambda s} \end{bmatrix}$ is a positive-definite matrix. Based on the above relations, the required voltage is determined as (8) and is forwarded to the two level symmetrical SVM modulator to produce the inverter switching pattern.

$$\begin{bmatrix} v_{\alpha s} \\ v_{\beta s} \end{bmatrix} = \begin{bmatrix} \frac{3}{2} n_P (i_{\beta s} + \frac{L_r}{\sigma L_m^2} \lambda_{\beta s}) & -\frac{3}{2} n_P (i_{\alpha s} + \frac{L_r}{\sigma L_m^2} \lambda_{\alpha s}) \\ 2\lambda_{\alpha s} & 2\lambda_{\beta s} \end{bmatrix}^{-1} \begin{bmatrix} -\frac{R_s + R_c}{R_c}(F_{tr} + \alpha_t \xi_1) \\ -\frac{R_s + R_c}{R_c}(\alpha_{\lambda s} \xi_2 + F_{\lambda s}) \end{bmatrix} \tag{8}$$

3. Stator Flux Observer

The stator flux vector is estimated in the stationary coordinate frame from

$$\underline{\boldsymbol{\lambda}}_{\mathbf{s}} = \int_0^t (\underline{\mathbf{v}}_{\mathbf{s}} - R_s \underline{\mathbf{i}}_{\mathbf{s}}) dt \tag{9}$$

According to (9), which is a main relation in the design of a big family of nonlinear IM drive controllers and observers, even small dc components in the voltage and current signals accumulate in the process of pure integration to form a large offset in the estimated stator flux vector components. It is clearly impossible to use these components in a nonlinear controller.

In this paper, the induced internal voltage of the induction motor ($\underline{\mathbf{v}}_{\mathbf{i}} = \underline{\mathbf{v}}_{\mathbf{s}} - R_s \underline{\mathbf{i}}_{\mathbf{s}}$) is initially integrated to form a virtual signal $\underline{\boldsymbol{\lambda}}_{\mathbf{1}}$. The average values of $\underline{\boldsymbol{\lambda}}_{\mathbf{1}}$ components ($<\underline{\boldsymbol{\lambda}}_{\mathbf{1}}>$) are computed using their period detection. The main frequency of the so-called components is determined from an indirect rotor flux field orientation scheme as

$$\omega = \omega_r + \omega_{slip}\ , \omega_{slip} = \frac{i_{qs}}{T_r i_{ds}} \tag{10}$$

where, ω_{slip} is the motor slip expressed in the Rotor Flux Orientation (RFO) frame and i_{ds}, i_{qs} are also the stator current vector components in the RFO frame. A contribution to the offset voltage vector ($\underline{\mathbf{v}}_{\mathbf{off}}$) is proposed as

$$\underline{\mathbf{v}}_{\mathbf{off}} = \frac{<\underline{\boldsymbol{\lambda}}_{\mathbf{s}}>}{T} \tag{11}$$

where, T indicates the total time that has elapsed.

One may note that due to the nonlinear distortion of the trajectory of $\underline{\boldsymbol{\lambda}}_{\mathbf{1}}$, the described algorithm is more an approximation. To improve on this, the signal $\underline{\mathbf{v}}_{\mathbf{off}}$ is low-pass filtered first and then fed back to the input of the integrator so as to cancel the offset components which exist in $\underline{\mathbf{v}}_{\mathbf{i}}$. This filtered value is subtracted from $\underline{\mathbf{v}}_{\mathbf{i}}$ and the result is again integrated to determine the offset compensated values of the stator flux components. It should be noted that a SM observer is employed for rotor flux vector detection which is required for the calculation of i_{ds} and i_{qs} components in (10).

It is worthwhile to mention that the phase voltage sensors are also eliminated to increase the system reliability and decrease the total cost of the IM drive. The phase voltages can be estimated from the dc link voltage and the inverter switching states (S_a, S_b, S_c)[18]. However, the switching patterns in our practical setup are available in the FPGA memory where they are applied to the PWM inverter with $1\mu s$ resolution (as is explained in section 7). To solve this problem, the average voltages of each phase in one sampling interval (5 kHz) are computed and employed using the sector number of the reference voltage space vector and the timing assignment of the SVM-PWM inverter which are available via the PC. One may note that the dc offset of the stator phase voltage sensors is perfectly eliminated using the mentioned method.

4. Rotor Flux and Rotor Speed Observer

The rotor flux observer of [19] is modified to simultaneously estimate the rotor flux space vector and rotor speed so that the PE condition is satisfied and no mechanical parameter is required. Suppose that the following rotor flux observer is available

$$\frac{d}{dt}\underline{\boldsymbol{\lambda}}_{\mathbf{r}} = \underline{\mathbf{f}}_{\boldsymbol{\lambda}\mathbf{r}} \quad , \quad \underline{\mathbf{f}}_{\boldsymbol{\lambda}\mathbf{r}} = [f_{\lambda\alpha}, f_{\lambda\beta}]^T \tag{12}$$

where the $\underline{\mathbf{f}}_{\boldsymbol{\lambda}\mathbf{r}}$ vector will be appropriately defined later. The following SM stator current observer is proposed

$$\frac{d}{dt}\hat{\underline{\mathbf{i}}}_{\mathbf{s}} = -\beta\underline{\mathbf{f}}_{\boldsymbol{\lambda}\mathbf{r}} + \frac{1}{\sigma L_s}(\underline{\mathbf{v}}_{\mathbf{s}} - R_s\underline{\mathbf{i}}_{\mathbf{s}}) + K_1\operatorname{sgn}(\tilde{\underline{\mathbf{i}}}_{\mathbf{s}}) \tag{13}$$

where $\beta = \frac{L_m}{\sigma L_s L_r}$ and sgn(.) denotes the sign function. According to [19], the vanishing of the estimate error vector $\tilde{\underline{\mathbf{i}}}_{\mathbf{s}} = \underline{\mathbf{i}}_{\mathbf{s}} - \hat{\underline{\mathbf{i}}}_{\mathbf{s}}$ is ensured by the sufficiently large gain K_1 of the discontinuous signal introduced to enforce a sliding mode behavior. The dynamics of the current estimation error are obtained as

$$\frac{d}{dt}\tilde{\underline{\mathbf{i}}}_{\mathbf{s}} = -\beta\frac{d}{dt}\tilde{\underline{\boldsymbol{\lambda}}}_{\mathbf{r}} - K_1\operatorname{sgn}(\tilde{\underline{\mathbf{i}}}_{\mathbf{s}}) \tag{14}$$

It is not possible to measure the rotor flux vector easily; hence, $\tilde{\underline{\boldsymbol{\lambda}}}_{\mathbf{r}} = \underline{\boldsymbol{\lambda}}_{\mathbf{r}} - \hat{\underline{\boldsymbol{\lambda}}}_{\mathbf{r}}$ must be substituted equivalently. The auxiliary vector $\underline{\mathbf{z}}$ is introduced

$$\underline{\mathbf{z}} = \tilde{\underline{\mathbf{i}}}_{\mathbf{s}} + \beta\tilde{\underline{\boldsymbol{\lambda}}}_{\mathbf{r}} = [z_\alpha, z_\beta]^T \tag{15}$$

which exhibits the following dynamics

$$\frac{d}{dt}\underline{\mathbf{z}} = -K_1\operatorname{sgn}(\tilde{\underline{\mathbf{i}}}_{\mathbf{s}}) \tag{16}$$

Based on (15), the vector of the rotor flux estimate error can be rewritten as

$$\tilde{\underline{\boldsymbol{\lambda}}}_{\mathbf{r}} = \frac{1}{\beta}(\underline{\mathbf{z}} - \tilde{\underline{\mathbf{i}}}_{\mathbf{s}}) \tag{17}$$

Relying on the knowledge of distinctive vectors $\underline{\boldsymbol{\lambda}}_{\mathbf{r}}$ and $\underline{\mathbf{i}}_{\mathbf{s}}$, it is now possible to define the $\underline{\mathbf{f}}_{\boldsymbol{\lambda}\mathbf{r}}$ vector so that the flux observer (12) can be rewritten as

$$\frac{d}{dt}\hat{\underline{\boldsymbol{\lambda}}}_{\mathbf{r}} = \underline{\mathbf{f}}_{\boldsymbol{\lambda}\mathbf{r}} = -\alpha(\hat{\underline{\boldsymbol{\lambda}}}_{\mathbf{r}} - L_m\underline{\mathbf{i}}_{\mathbf{s}}) + j\,\hat{\omega}_r\,\hat{\underline{\boldsymbol{\lambda}}}_{\mathbf{r}} + K_2\tilde{\underline{\boldsymbol{\lambda}}}_{\mathbf{r}} \tag{18}$$

where α and $\hat{\omega}_r$ show the rotor time constant inverse and estimated rotor speed, respectively. According to (18), the error dynamics of the flux estimate turn out to be

$$\frac{d}{dt}\tilde{\underline{\boldsymbol{\lambda}}}_{\mathbf{r}} = (j\,\omega_r - \alpha - K_2)\tilde{\underline{\boldsymbol{\lambda}}}_{\mathbf{r}} + j\,\tilde{\omega}_r\,\tilde{\underline{\boldsymbol{\lambda}}}_{\mathbf{r}} \tag{19}$$

Equation (19) becomes in matrix from

$$\dot{\tilde{\underline{\boldsymbol{\lambda}}}}_{\mathbf{r}} = P\tilde{\underline{\boldsymbol{\lambda}}}_{\mathbf{r}} + W^T\tilde{\boldsymbol{\omega}}_{\mathbf{r}}, \mathbf{P} = \begin{bmatrix} -\alpha - K_2 & -\omega_r \\ \omega_r & -\alpha - K_2 \end{bmatrix},$$
$$\mathbf{W}^{\mathbf{T}} = \begin{bmatrix} -\hat{\lambda}_{\beta r} \\ \hat{\lambda}_{\alpha r} \end{bmatrix} \tag{20}$$

The following Lyapunov function is selected

$$V_1 = \frac{1}{2}[\tilde{\underline{\lambda}}_r^{\mathbf{T}} \tilde{\underline{\lambda}}_r + \gamma_\omega^{-1} \tilde{\omega}_r^2] \tag{21}$$

in which, $\gamma_\omega > 0$.

The time derivation of V_1 is expressed as

$$\dot{V}_1 = \tilde{\underline{\lambda}}_r^{\mathbf{T}} (\mathbf{P} \tilde{\underline{\lambda}}_r + \mathbf{W}^{\mathbf{T}} \tilde{\omega}_r) + \gamma_\omega^{-1} \tilde{\omega}_r \dot{\tilde{\omega}}_r \tag{22}$$

Assuming the adaptation law as

$$\dot{\tilde{\omega}}_r = -\gamma_\omega \mathbf{W} \tilde{\underline{\lambda}}_r \tag{23}$$

Then,

$$\dot{V}_1 = \tilde{\underline{\lambda}}_r^{\mathbf{T}} \mathbf{P} \tilde{\underline{\lambda}}_r \leq 0 \tag{24}$$

From the above result

$$V_1(t) - V_1(0) = \int_0^t -(\alpha + K_2)(\tilde{\lambda}_{\alpha r}^2 + \tilde{\lambda}_{\beta r}^2) d\tau > L \tag{25}$$

where, L is a finite negative constant and as a result, $\tilde{\underline{\lambda}}_r \in L_2$.

On the other hand, V_1 is a radially unbounded function; therefore, it is guaranteed that $\tilde{\underline{\lambda}}_r$ and $\tilde{\omega}_r$ are bounded ($\tilde{\underline{\lambda}}_r, \tilde{\omega}_r \in L_\infty$). Rotor speed ($\omega_r$) can be assumed as an unknown constant parameter because the sampling time is considered to be small enough. As a result, $\dot{\hat{\omega}}_r = -\dot{\tilde{\omega}}_r$ and $\hat{\omega}_r$ is also bounded. In addition, since $\underline{\lambda}_r$ is assumed to be bounded, the estimated rotor flux vector is also bounded. As a consequence, considering (20), W^T and $\dot{\tilde{\underline{\lambda}}}_r$ must be bounded. Considering the above discussion and using Barbalat's lemma, it follows that

$$\lim_{t \to \infty} \tilde{\underline{\lambda}}_r = 0 \tag{26}$$

Furthermore, the PE lemma implies that if $\mathbf{W}$ and $\dot{\mathbf{W}}$ are uniformly restricted and the PE condition is satisfied, i.e. there exists some T>0 such that for any t>0, $\int_t^{t+T} \mathbf{W}(\tau)\mathbf{W}^{\mathbf{T}}(\tau) d\tau > 0$, then the parameter estimation error $\tilde{\omega}_r$ will also converge to zero [7]. Relying on (18), $\frac{d}{dt}\hat{\lambda}_{\alpha r}$ and $\frac{d}{dt}\hat{\lambda}_{\beta r}$ are confined signals and, therefore, $\frac{d}{dt}\mathbf{W}$ is also bounded. Moreover,

$$\begin{aligned} \int_t^{t+T} \mathbf{W}(\tau)\mathbf{W}^{\mathbf{T}}(\tau) d\tau &= \int_t^{t+T} \begin{bmatrix} -\hat{\lambda}_{\beta r}(\tau) & \hat{\lambda}_{\alpha r}(\tau) \end{bmatrix} \begin{bmatrix} -\hat{\lambda}_{\beta r}(\tau) \\ \hat{\lambda}_{\alpha r}(\tau) \end{bmatrix} \\ &= \int_t^{t+T} (\hat{\lambda}_{\alpha r}^2 + \hat{\lambda}_{\beta r}^2) d\tau > 0 \end{aligned} \tag{27}$$

As a result, rotor speed estimation is correctly achieved using the so-called SM observer.

5. Stator and Rotor Resistances Estimation

Stator and rotor resistances of the induction motor are also estimated through the following RLS method. In order to apply the RLS technique, the model must be written in the form of

$$y(t) = \boldsymbol{\varphi}^{\mathbf{T}}(\mathbf{t})\boldsymbol{\theta} \tag{28}$$

where, y(t) is an arbitrary observable quantity, $\boldsymbol{\theta}$ is the vector of unknown parameters to be estimated and $\boldsymbol{\varphi}(\mathbf{t})$ is the vector of known functions which depends on other definite variables. The model is indexed by variable t, which often denotes time [20].

Consider the following cost function

$$J = \frac{1}{2}\Sigma[y(t) - \boldsymbol{\varphi}^{\mathbf{T}}(\mathbf{t})\boldsymbol{\theta}]^2 \tag{29}$$

In the RLS method, the cost function of (29) can be minimized by updating the estimated vector through the following recursive procedure [20,21]

$$\begin{aligned} \hat{\boldsymbol{\theta}}(\mathbf{t}) &= \hat{\boldsymbol{\theta}}(\mathbf{t-1}) + \mathbf{L}(\mathbf{t})(y(t) - \boldsymbol{\varphi}^{\mathbf{T}}(\mathbf{t})\hat{\boldsymbol{\theta}}(\mathbf{t-1})) \\ \mathbf{L}(\mathbf{t}) &= \mathbf{P}(\mathbf{t-1})\boldsymbol{\varphi}(\mathbf{t})(\mathbf{I} + \boldsymbol{\varphi}^{\mathbf{T}}(\mathbf{t})\mathbf{P}(\mathbf{t-1})\boldsymbol{\varphi}(\mathbf{t}))^{-1} \\ \mathbf{P}(\mathbf{t}) &= (\mathbf{I} - \mathbf{L}(\mathbf{t})\boldsymbol{\varphi}^{\mathbf{T}}(\mathbf{t}))\mathbf{P}(\mathbf{t-1}) \end{aligned} \tag{30}$$

where, **I** is the identity matrix with appropriate dimensions and **P(t)** is a positive definite matrix, which initially can be selected as a positive multiple of the unity matrix.

In the model of (28), the vector of unknown parameters is assumed to be constant, but in several cases such as electrical machines, parameters may vary. To solve this problem, two techniques have been suggested. The first is to use a discount factor or forgetting factor, while the second is to reset the matrix **P(t)** alternatively with a diagonal matrix with large elements [21]. It is worthwhile to mention that the second method is employed in this research work.

Considering the IM equivalent circuits in the stationary reference frame, one can obtain

$$v_{\alpha s}=R_s i_{\alpha s}+L_{ls}\dot{i}_{\alpha s}-\omega_r\lambda_{\beta r}-L_{lr}\dot{i}_{\alpha r}-R_r i_{\alpha r}$$
$$=R_s i_{\alpha s}+L_{ls}\dot{i}_{\alpha s}-\omega_r\phi_{\beta r}-(L_{lr}\frac{d}{dt}+R_r)\frac{1}{L_r}(\lambda_{\alpha r}-L_m i_{\alpha s}) \quad (31)$$

One may note that $\lambda_{\alpha r}$ and $\lambda_{\beta r}$ are determined from the rotor flux SM observer described before while $v_{\alpha s}$ and $i_{\alpha s}$ are calculated from the estimated stator voltages and the measured stator currents. Based on (31), it is possible to introduce

$$y(t)=v_{\alpha s}(t)-L_{ls}\dot{i}_{\alpha s}+\omega_r\lambda_{\beta r}+L_{lr}\frac{d}{dt}[\frac{1}{L_r}(\lambda_{\alpha r}-L_m i_{\alpha s})]$$
$$\varphi^T(t)=\begin{bmatrix} i_{\alpha s} & \frac{1}{L_r}(\lambda_{\alpha r}-L_m i_{\alpha s})\end{bmatrix}, \quad \theta^T=\begin{bmatrix}\hat{R}_s & \hat{R}_r\end{bmatrix} \quad (32)$$

At this stage, the method can be applied to estimate the motor resistances. To solve the problem of derivatives in (32), the following first order low pass filter is proposed

$$H(s)=\frac{1}{s+a} \quad (33)$$

where, a is the cutoff frequency of the so-called filter. Using this filter for example becomes

$$\frac{s}{s+a}i_{\alpha s}=i_{\alpha s}-a i_{\alpha sf} \quad (34)$$

where, denotes the filtered value of $i_{\alpha s}$.

6. Simulation Results

Based on the described control theory, the overall block diagram of an IM drive is shown in Fig. 2.

A C^{++} computer program was developed to model the whole system shown in Fig. 2. In this program, the system equations are solved to obtain the system state variables, using the static fourth order Runge-Kutta numerical method. Simulation results were obtained for a three-phase squirrel cage induction motor with characteristics given in Table 1.

Table 1. Induction motor specification.

$n_P=2$	$N_r=1430$r/min
$V_s=380$v	$I_s=4.9$A
$L_{ls}=L_{lr}=16$mH	$L_m=328$mH
$R_s=3.6\,\Omega$	$R_r=1.88\ \Omega$

The results obtained for IM direct torque control and speed control are respectively shown in Figs. 3, 4. One may note that a conventional PI controller is used to generate the torque reference signal in the case of the speed control.

Direct torque control with a step up/down torque reference and a constant flux reference of 0.4 Wb-turn is shown in Fig. 3. Four quadrant speed control of the IM drive with the same constant flux reference of 0.4 Wb-turn is also depicted in Fig. 4.

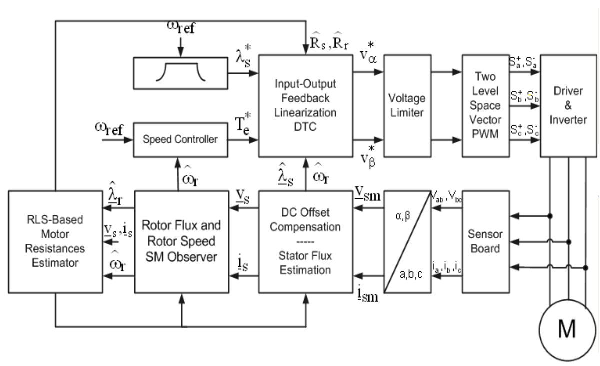

Fig. 2. Proposed IM DTC-SVM control block diagram.

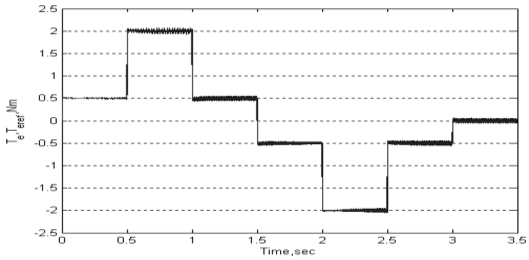

(a) Motor torque

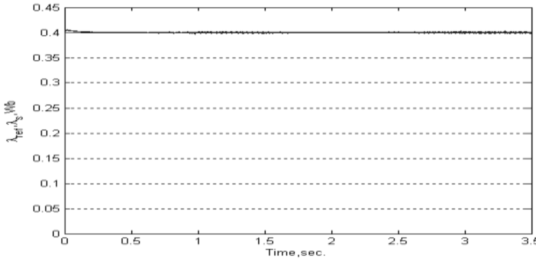

(b) Stator flux

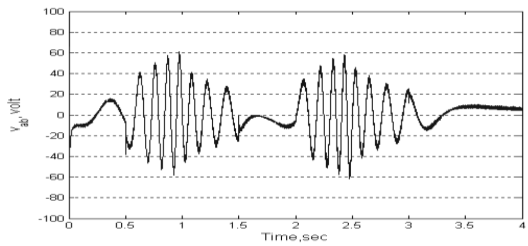

(c) Stator voltage

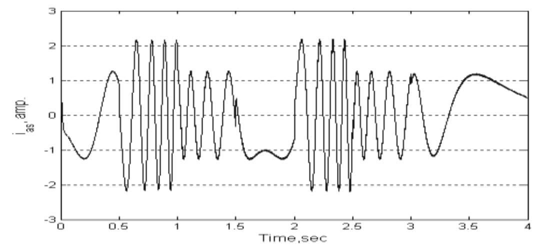

(d) Stator current

Fig. 3. Simulation Results, IM direct torque control.

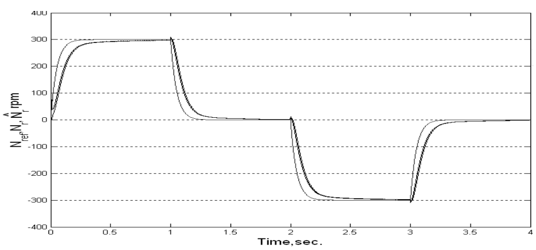

(a) Motor speed

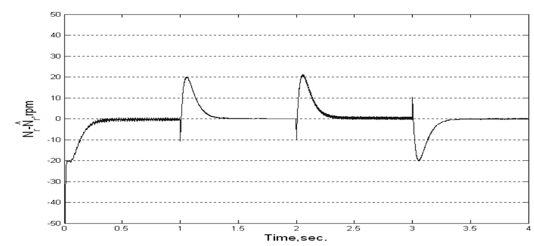

(b) Speed estimation error

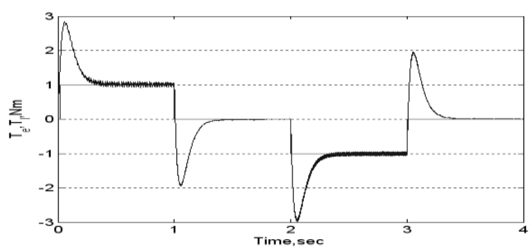

(c) Motor and load torque

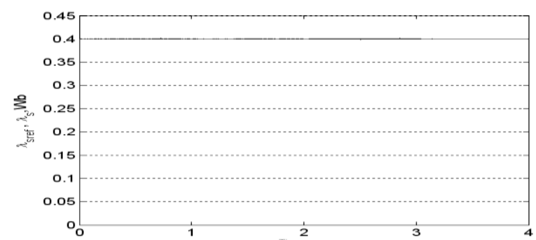

(d) Stator flux

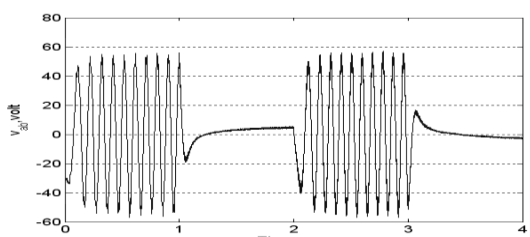

(e) Stator voltage

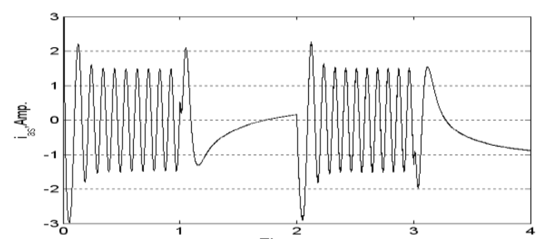

(f) Stator current

Fig. 4. Simulation Results, IM speed control.

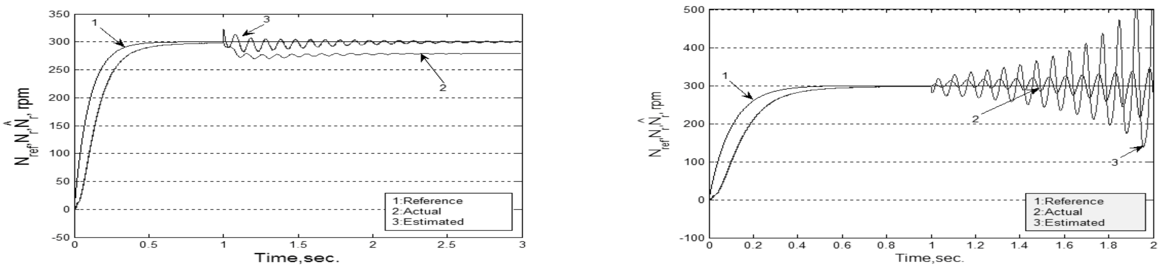

(a) with fifty percent increment (b) with fifty percent decrement

Fig. 5. Simulation Results, IM speed control under motor resistances variation.

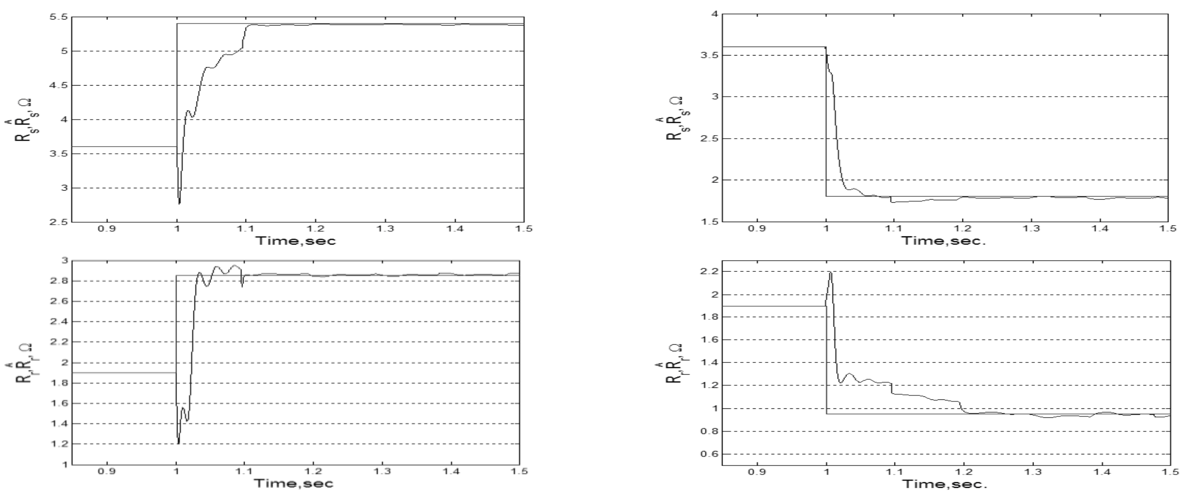

(a) with +50% increment (b) with -50% decrement

Fig. 6. Simulation Results and Motor resistances estimation.

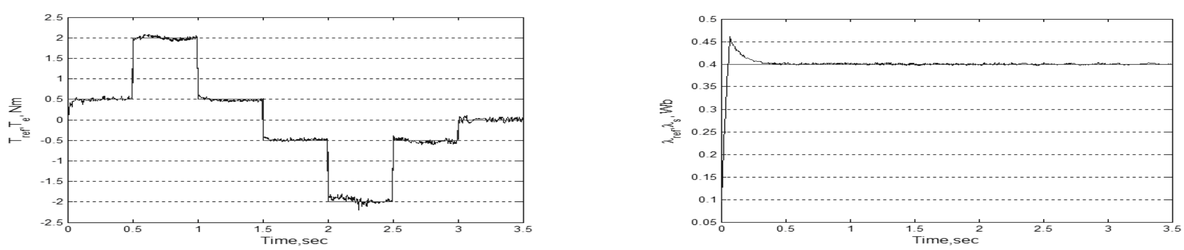

(a) Motor torque (b) Stator flux

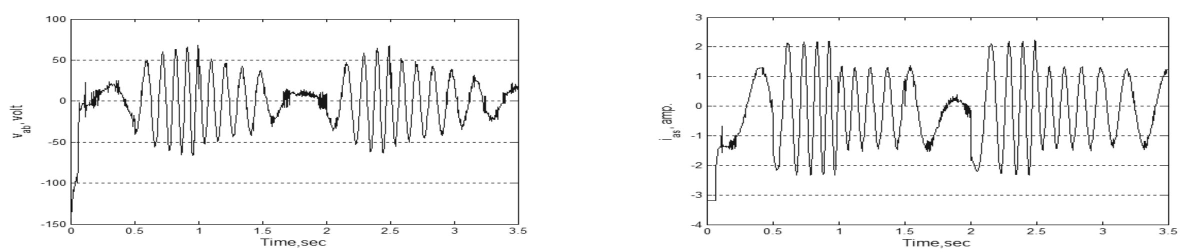

(c) Stator voltag (d) Stator current

Fig. 8. Experimental Results and IM direct torque control.

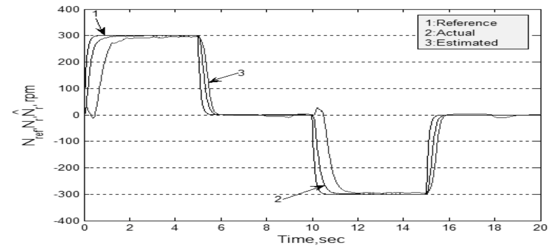

(a) Motor speed

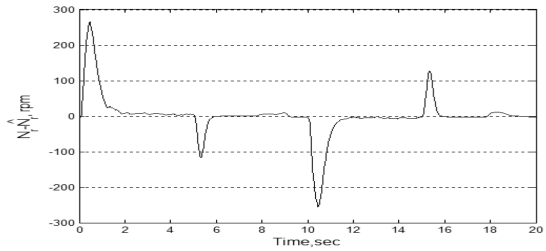

(b) Speed estimation error

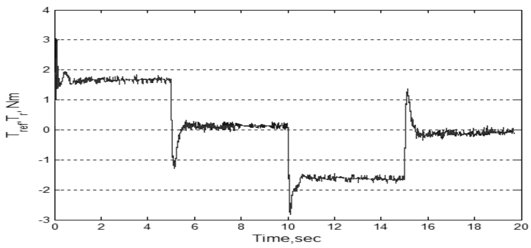

(c) Motor torque

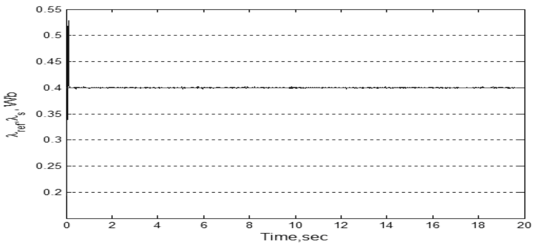

(d) Stator flux

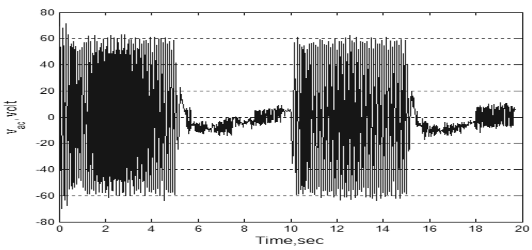

(e) Stator voltage

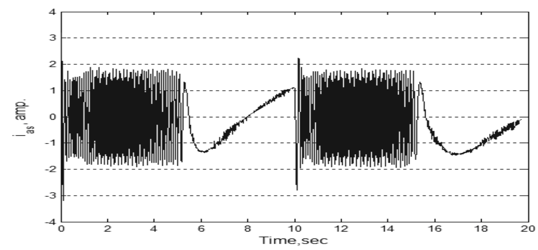

(f) Stator current

Fig. 9. Experimental Results and IM speed control.

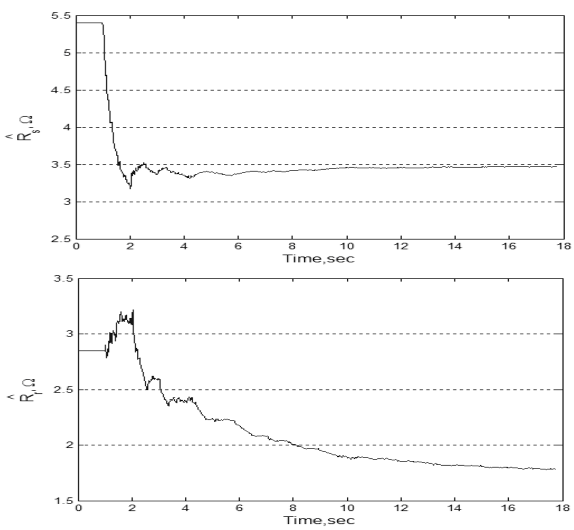

(a) with +50% initial overestimation

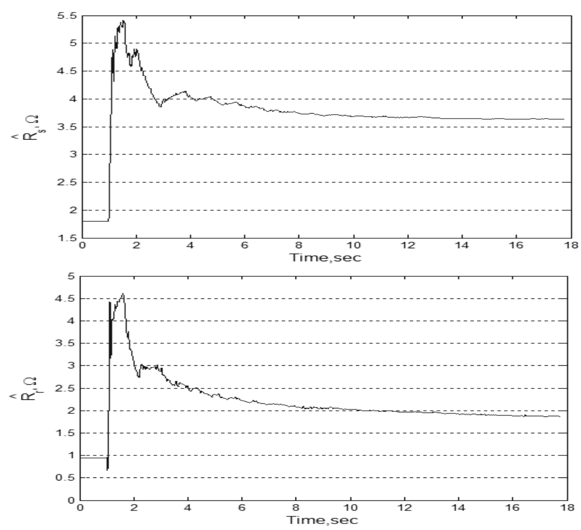

(b) with -50% initial underestimation

Fig. 10. Experimental Results and Motor resistances estimation.

As can be seen from these figures, a fast tracking of stator flux and motor torque/motor speed is achieved. Speed control of an IM drive with ±50% variation of stator and rotor resistances respective to their nominal values is also shown in Fig. 5. It shows that the speed tracking and even the drive stability is lost under these conditions.

Stator and rotor resistance estimation using the proposed RLS observer and assuming ±50% step variation is depicted in Fig. 6. This figure shows that a fast and almost precise tracking of the so-called parameters of an IM drive has been achieved.

7. Experimental Results

For practical evaluation of the actual system performance, a PC-based prototype system has been built and tested. The experimental setup according to the overall system block diagram shown in Fig. 2 is depicted in Fig. 7 and consists of the following sections:

a 2.5kw squirrel cage induction motor and a 2.5kw DC generator as its load; a three-phase voltage source inverter and its isolation board; a DC voltage and current sensors board; a 96 bit digital Input-Output card; a 32-channel A/D converter card; an FPGA board and a PC for calculating the required computations of the proposed ideas signals and monitoring the registered waveforms.

The induction motor is supplied with a three-phase PWM inverter which employs the symmetrical two level space vector modulation. A Xilinx XC95288xl FPGA has been selected for real-time implementation of switching patterns using a switching frequency of 5 kHz.

The FPGA board communicates with the PC via the digital Advantech PCI-1753 I/O board. The FPGA in the experimental setup accomplishes the following tasks: switching pattern generation of IGBT switches based on symmetrical SVM technique, providing a useful dead time for power switches in the so-called switching patterns, generation of the synchronizing signal for data transmission between PC and hardware and shutting down the inverter in the case of emergency conditions such as over current or PC hanging states.

The inverter has been designed and implemented specifically for this experiment using an SKM75 GD 124 D SEMIKRON module. The required drive board has been designed using HCPL 316J which is a fast and intelligent IGBT driver and guarantees a reliable isolation between the high voltage and control boards.

DC link voltage and stator phase currents are measured by Hall-type LEM sensors. All measured electrical signals are filtered using separate analogue second order low pass filters and then converted to digital signals using a 12-bit A/D card with 10μs conversion time.

The motor speed is measured for comparison with its estimated value using an AUTONICS incremental encoder with 1024 pulses per round. The output of the speed sensor is sent to a 89c2051 microcontroller whose output is forwarded to the PC via I/O card. A low pass filter is also implemented in the PC to omit the high frequency noise on the measured and estimated speed.

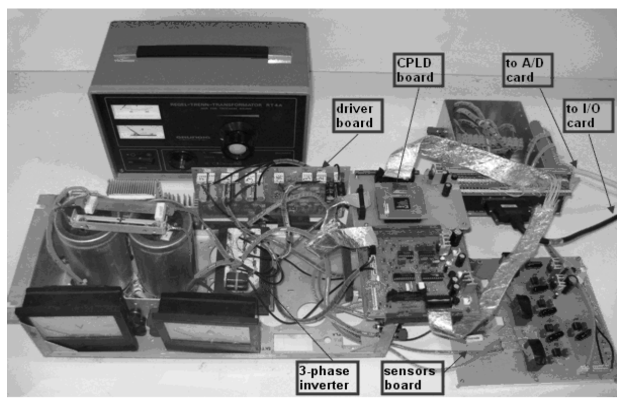

Fig. 7. Experimental setup.

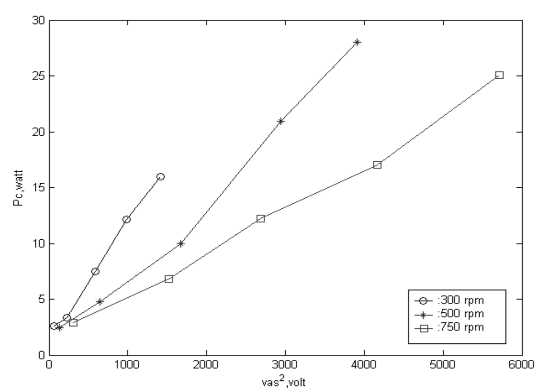

Fig. 11. IM iron losses.

The validity and effectiveness of the proposed control approach is shown by adopting the same objectives as the simulation results. The controller and observer gains are nearly the same as used in the system simulation. The experimental results obtained for the IM direct torque control, speed control and motor resistances estimation are respectively shown in Figs. 8-10. A close agreement is considered between these results and those of Figs. 3-6.

It is worthwhile to mention that the iron losses equivalent resistance (R_c) of induction motor at some rotor speeds has been determined using a useful method. The DC machine was employed as a no-load DC generator with a fixed field excitation while the IM was driven with a constant speed. The effective values of voltage and current signals accompanied by motor input power which is composed of IM core and copper losses, DC generator core losses and mechanical losses are computed. The above test was performed for various stator flux reference values for each fixed speed.

The induction motor copper losses in each test can be simply computed from the effective value of the stator current while the combined value of the DC machine core losses and mechanical losses was determined by the DC machine drive as a DC motor with the same values of stator voltage and rotor speed. As a result, the IM core losses can be calculated as a function of the stator effective voltage which has been shown in Fig. 11 for $\frac{1}{5}, \frac{1}{3}$ and half of the IM rated speed. Stator core losses equivalent resistance was determined from these results and was employed in both simulation and experimental results.

8. Conclusions

A sensorless DTC-SVM method has been described for three-phase IM drives which is based on an input-output feedback linearization technique. The motor iron loss has been taken into account using a speed dependent shunt resistance. This resistance was determined through an appropriate experimental test. A novel method is also presented for DC offset compensation which is a major problem of stator flux vector estimation through pure integration. A SM rotor flux observer is developed for simultaneous estimation of rotor flux space vector and rotor speed. A RLS-based estimator is also proposed for simultaneous detection of stator and rotor resistances. The capabilities of the proposed nonlinear control approaches have been examined and verified by both simulation and experimental results. A little disagreement observed between these two sets of results can be explained with inaccuracies which exist in the current and voltage signals acquisition, gain unbalances of the voltage and current acquisition channels, inaccurate IGBT models in the simulation results and, finally, because of the IM magnetic saturation that is not taken into account in the simulation results.

References

[1] M. Salem, "Classical controller with intelligent properties for speed control of vector controlled induction motor," *Journal of Power Electronics*, Vol. 8, No. 3, pp. 210-216, 2008.

[2] J.A. Santisteban, R.M. Stephan, "Vector control methods for induction machines: an overview," *IEEE Trans. on Edu*., Vol. 44, pp.170-175, 2001.

[3] L. Hong, et al., "Implementation of direct torque control using matrix converter fed induction motor," *Journal of Power Electronics*, Vol. 8, No.1, pp. 74-80, 2008.

[4] M. Bertoluzzo, et al., "Direct torque control of an induction motor using a single current sensor," *IEEE Trans. on Ind. Elec.*, Vol. 53, pp. 778-784, 2006.

[5] V. Ambrozic, et al., "Band-constrained technique for direct torque control of induction motor," *IEEE Trans. on Ind. Elec.*, Vol. 51, pp. 776-784, Aug. 2004.

[6] S. Kaboli, E. Vahdati-Khajeh, M.R. Zolghadri, "Probabilistic voltage harmonic analysis of direct torque controlled induction motor drives," *IEEE Trans. on Pow. Elec.*, vol. 21, July 2006, pp: 1041-1052.

[7] G. R. Arab, J. Soltani, "Robust direct torque control of adjustable speed sensorless induction machine drive based on space vector modulation using a PI predictive controller," *Springer*, pp. 485-496, 2006.

[8] J. Rodriguez, et al., "Simple direct torque control of induction machine using space vector modulation," *Elec. Let.*, Vol. 40, pp. 412-413, April 2004.

[9] C. Lascu, et. al., "Direct torque control of sensorless induction motors: A sliding mode approach," *IEEE Trans. on Ind. App.*, Vol. 40, pp. 582-590, March/April 2004.

[10] A. Benchaib, et. al., "Sliding mode input-output linearization and field orientation for real-time control of induction motors," *IEEE Trans on Pow. Elec.*, Vol. 14, pp. 3-13, Jan. 1999,.

[11] K.C. Veluvolu, et. al., "Robust observer with sliding mode estimation for nonlinear uncertain systems," *Control Theory & Applications*, Vol. 1, pp. 1533-1540, Sept. 2007.

[12] J. Holtz, et. al., "Drift and parameter compensated flux estimator for persistent zero stator frequency operation of sensorless controlled induction motors," *IEEE Trans. on Ind. App.*, pp. 1052-1060, July 2003.

[13] J. Hu, et. al., "New integration algorithms for estimating motor flux over a wide speed range," *IEEE Trans. Pow. Elec.*, Vol. 13, pp. 969-977, Sept. 1998.

[14] M. Barut, et. al., "Experimental evaluation of braided EKF for sensorless control of induction motors," *IEEE Trans. on Ind. Elec.*, Vol. 55, pp.620-632, Feb. 2008.

[15] J. Soltani, M. Hajian, "Adaptive fuzzy sliding mode control of speed sensorless universal field oriented induction motor drive with on-line stator resistance tuning," *Iranian Journal of Science & Technology*, Vol. 29, Trans. B., 2005.

[16] B.Karanayil, et al., "Online stator and rotor resistance estimation scheme using artificial neural networks for vector controlled speed sensorless induction motor drive," *IEEE Trans. on Ind. Elec.*, Vol. 54, pp.167-176, Feb. 2007,.

[17] I. Boldea, et. al., *The induction machine handbook*, CRC Press, Chapter 13, 2002.

[18] L.S. Xuefang, et al., "Implementation of hybrid control for motor drives," *IEEE Trans. on Ind. Elec.*, Vol. 54, pp. 1946-1952, Aug. 2007.

[19] C. Aurora, et al., "Design and experimental test of a speed/flux sliding mode observer for sensorless induction motors," *in Proc. of American Control Conf.*, pp. 5881-5886, July 2007.

[20] N.R. Abjadi, et. al., "Adaptive control of doubly fed field-oriented induction machine based on recursive least squares method taking the iron loss into account," *in Proc. of IPEMC2006*, pp. 1-5, Aug. 2006.

[21] K.J. Astrom, et. al., *Adaptive control*, Addison-Wesley Longman Publishing Co., 2nd Ed., 1994.

Masood Hajian (1978) graduated from Sharif University of Technology, Iran and obtained his Master's degree from Isfahan University of Technology, Isfahan/Iran. His main area of research is power electronics and drives. He was with the Electrical and Computer Research Center of Isfahan University of Technology, Isfahan/Iran from 2002 to 2004. He is presently a PhD student on the faculty of the Electrical and Computer Engineering department in Isfahan University of Technology.

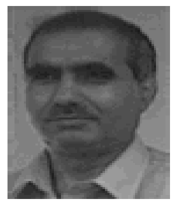

Jafar Soltani (1951) graduated from Tabriz University, Tabriz/Iran. He holds a Master's and a Ph.D degree from UMIST. He is a professor emeritus of Isfahan University of Technology, Isfahan/Iran. His main area of research is electrical machines and drives. He is a member of the IEEE.

Gholamreza Arab Markadeh was born in Shahrekord, Iran in 1974. He received the BSc, MS and PhD degrees from Isfahan University of Technology, Isfahan, Iran, both in Electrical Engineering, respectively, in 1996, 1998 and 2005. He is currently on the faculty of the engineering department of Shahrekord University, Shahrekord, Iran. His fields of research are nonlinear control, power electronics and variable-speed ac drives.

Saeed Hosseinnia received the M.S. degree from Oklahoma State University, Stillwater, USA in 1974 and the Ph.D. degree from Isfahan University of Technology, Isfahan, Iran in 1999 both in Electrical Engineering. Since 1985, he has been with Isfahan University of Technology where he is currently an assistant professor of Electrical Engineering. His research interests include system theory, nonlinear control and robust control.